

Quantitative Analysis of Shock Wave Dynamics in a Fluid of Light

T. Bienaimé, M. Isoard, Q. Fontaine, A. Bramati, A. M. Kamchatnov, Quentin Glorieux, N. Pavloff

▶ **To cite this version:**

T. Bienaimé, M. Isoard, Q. Fontaine, A. Bramati, A. M. Kamchatnov, et al.. Quantitative Analysis of Shock Wave Dynamics in a Fluid of Light. Physical Review Letters, 2021, 126 (18), pp.183901. 10.1103/PhysRevLett.126.183901 . hal-03644007

HAL Id: hal-03644007
https://hal.science/hal-03644007

Submitted on 17 Apr 2022

HAL is a multi-disciplinary open access archive for the deposit and dissemination of scientific research documents, whether they are published or not. The documents may come from teaching and research institutions in France or abroad, or from public or private research centers.

L'archive ouverte pluridisciplinaire **HAL**, est destinée au dépôt et à la diffusion de documents scientifiques de niveau recherche, publiés ou non, émanant des établissements d'enseignement et de recherche français ou étrangers, des laboratoires publics ou privés.

Quantitative Analysis of Shock Wave Dynamics in a Fluid of Light

T. Bienaimé,[1] M. Isoard,[2,3] Q. Fontaine,[1] A. Bramati,[1] A. M. Kamchatnov,[4,5] Q. Glorieux,[1] and N. Pavloff[2]
[1]Laboratoire Kastler Brossel, Sorbonne Université, CNRS, ENS-PSL Research University, Collège de France, Paris 75005, France
[2]Université Paris-Saclay, CNRS, LPTMS, 91405 Orsay, France
[3]Physikalisches Institut, Albert-Ludwigs-Universität Freiburg, Hermann-Herder-Straße 3, D-79104 Freiburg, Germany
[4]Moscow Institute of Physics and Technology, Institutsky lane 9, Dolgoprudny, Moscow region 141700, Russia
[5]Institute of Spectroscopy, Russian Academy of Sciences, Troitsk, Moscow 108840, Russia

(Received 2 February 2021; accepted 2 April 2021; published 5 May 2021)

We report on the formation of a dispersive shock wave in a nonlinear optical medium. We monitor the evolution of the shock by tuning the incoming beam power. The experimental observations for the position and intensity of the solitonic edge of the shock, as well as the location of the nonlinear oscillations are well described by recent developments of Whitham modulation theory. Our work constitutes a detailed and accurate benchmark for this approach. It opens exciting possibilities to engineer specific configurations of optical shock wave for studying wave-mean flow interaction.

DOI: 10.1103/PhysRevLett.126.183901

In many different fields such as acoustics [1], plasma physics [2], hydrodynamics [3–5], nonlinear optics [6], ultracold quantum gases [7–10], the short time propagation of slowly varying nonlinear pulses can be described discarding the effects of dispersion and dissipation. The prototype of such an approach is given by the system of equations governing compressible gas dynamics [11]. This type of treatment typically predicts that, due to nonlinearity, an initially smooth pulse steepens during its time evolution, eventually reaching a point of gradient catastrophe. This is the wave-breaking phenomenon, which results in the formation of a shock wave [12,13]. If, after wave breaking, dispersive effects dominate over viscosity, the shock eventually acquires a stationary nonlinear oscillating structure for which the width increases with diminishing dissipation [14]. In the case of weak dissipation the time for reaching a stationary regime can be quite long. Gurevich and Pitaevskii [15] made a major contribution to the field when they first realized the interest of studying the evolution of the associated dynamical structure, now called a dispersive shock wave (DSW). Besides, they understood that a DSW can be described as a modulated nonlinear traveling wave and studied in the framework of the Whitham theory of modulations [16].

In the present work we study the propagation of an optical beam in a nonlinear defocusing medium. Wave-breaking and (spatial or temporal) dispersive shocks have already been observed in such a setting [17–30]. However, all previous theoretical descriptions of experimental optical shocks either remained only qualitative or resorted to numerical simulations for reaching accurate descriptions. Indeed, a realistic quantitative characterization of the experimental situation requires to take into account a number of nontrivial effects which sum up to a quite difficult task. For instance, saturation effects, such as occurring in semiconductor doped glasses [31] and in photorefractive media [32], can only be taken into account by using a nonintegrable nonlinear equation, even for a medium with a local nonlinearity. Besides, both "Riemann invariants" typically vary during the prebreaking period and this complicates the description of the nondispersive stage of the pulse spreading, even in a quasi unidimensional (1D) geometry. Moreover, for realistic initial intensity pulse profiles, the post-breaking evolution corresponds, at best, to a so-called "quasisimple" dispersive shock [33], the characterization of which requires an elaborate extension of the Gurevich-Pitaevskii scheme. Finally, the nonintegrability of the wave equation significantly complicates the post-breaking description of the nonlinear oscillations within the shock. Despite these difficulties, it has recently become possible to combine several theoretical advances [34–45] to obtain a comprehensive treatment of the nonlinear pulse spreading and the subsequent formation of a dispersive shock in a realistic setting [46,47]. In this Letter, we provide a nonambiguous experimental evidence for the accuracy of this theory with a precise description of the main features of the shock. This universal and quantitative benchmark is a major advance for manipulation and engineering of optical shockwaves.

We study the propagation of a laser field in a $L = 7.5$ cm-long cell filled with an isotopically pure ^{85}Rb vapor (99% purity) warmed up to a controlled temperature of 120 °C to adjust the atomic vapor density. We use a Ti:sapphire laser detuned by -3.9 GHz with respect to the $F = 3 \to F'$ transition of the D2-line of ^{85}Rb at $\lambda_0 = 2\pi/k_0 = 780$ nm. For such a large detuning, the natural Lorentzian shape of the line dominates and the Doppler broadening $k_0 v \simeq 240$ MHz can be safely

 © 2021 American Physical Society

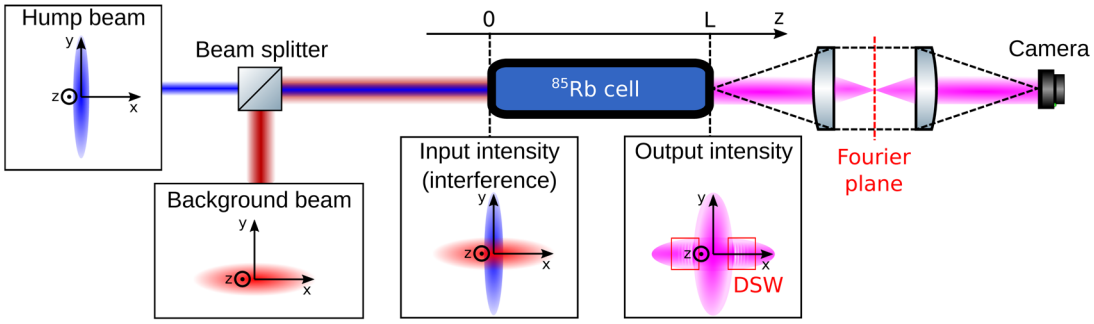


FIG. 1. Sketch of the experimental setup. To create the initial state we overlap the background and the hump beams on a beam splitter with their relative phase precisely adjusted such that they interfere constructively. This state then propagates inside the nonlinear medium consisting of a hot ^{85}Rb vapor cell of length L. The insets represent cuts of the relevant intensity profiles in the plane perpendicular to the direction z of propagation. The output intensity is recorded on a camera by direct imaging through two lenses in $4f$ configuration.

neglected. In these experimental conditions, the system is self defocusing (repulsive photon-photon interaction) and the transmission through the cell is 60%. We find that this medium is well described by local photon-photon interactions, but contrary to previous works [48–52] we find it important to take into account the saturation of the nonlinearity to quantitatively describe the dynamics of the shock waves.

The input intensity profile is a cross-beam configuration of two vertically polarized laser beams, both propagating along the axis of the cell (denoted as Oz), with their respective phase precisely adjusted such that the two beams interfere constructively, see Fig. 1. One of the beams (which is denoted the *hump*) is extended along the y direction and significantly more intense than the other one (the *background*) which is extended along the x direction. At the entrance of the cell ($z = 0$) both beams have an elliptic Gaussian profile. The background beam has a power P_0 and waists $w_{x,0} > w_{y,0}$, whereas the hump has power P_1 and waists $w_{x,1} < w_{y,1}$; see Supplemental Material [53]. During the initial nondiffractive stage of evolution, nonlinearity acts as an effective pressure which favors spreading of the hump in the x direction along which is initially tighter collimated. Conversely, the low intensity background experiences almost no spreading and behaves as a pedestal which triggers wave breaking of the hump during its spreading. Each beam has a maximum entrance intensity $\mathcal{I}_\alpha = 2P_\alpha/(\pi w_{x,\alpha} w_{y,\alpha})$ ($\alpha = 0$ or 1), and we explore the DSW dynamics for a fixed ratio $\mathcal{I}_1/\mathcal{I}_0$. We work in the deep nonlinear regime, with $\mathcal{I}_1 = 20\mathcal{I}_0$. This large value corresponds to a wave breaking distance typically shorter than the cell length, and makes it possible, by changing the total power $P_{\rm tot}$ of the beams, to observe several stages of evolution of the DSW. The total power can be increased up to 700 mW and is limited by the laser maximum output power.

We image the total field intensity $I_{\rm out}(x, y)$ at the output of the cell on a camera. In order to minimize the effect of absorption and increase the visibility of the DSW, we determine the *normalized* output intensity

$$\tilde{I}_{\rm out}(x, y) \equiv \frac{I_{\rm out}(x, y) - I^0_{\rm out}(x, y)}{\mathcal{I}^0_{\rm out}}, \tag{1}$$

where $I^0_{\rm out}(x, y)$ is the intensity profile at the cell output when *only* the background beam propagates through the medium (the hump beam is blocked). $\mathcal{I}^0_{\rm out}$ is the maximal value of $I^0_{\rm out}(x, y)$. $\tilde{I}_{\rm out}(x, y)$ is represented in Fig. 2(a). Our theoretical description relies on only two parameters which characterize the photon-photon interaction, namely, the Kerr coefficient, n_2, and the saturation intensity $I_{\rm sat}$ [cf. Eq. (2)]. Their values $n_2 = 1.5 \times 10^{-4}$ mm^2/W, and $I_{\rm sat} = 0.6$ W/mm^2 have been determined by comparing the experimental results with large-scale 2D numerical simulations [53]. The excellent agreement reached in Fig. 2 indicates that two effects—saturable nonlinearity and linear absorption—are the relevant physical ingredients for a theoretical description of our experiment.

In the regime $w_{1,x} \ll w_{0,x}$ and $\mathcal{I}_1 \gg \mathcal{I}_0$ we consider, the normalized output density $\tilde{I}_{\rm out}$ becomes independent on the precise shape of the background beam. As a result, $\tilde{I}_{\rm out}(x, 0)$ can be described by using a simplified 1D theoretical description, where a hump propagates over a background of *uniform* intensity $\mathcal{I}_0$. Within the cell, the complex field amplitude at $y = 0$, denoted as $\mathcal{A}(x, 0, z) \equiv a(x, z)$, then obeys a 1D nonlinear Schrödinger equation where the position z along the axis of the beam plays the role of an effective "time" [61]. The equation, once included the nonlinearity saturation and the linear absorption [32], reads

$$i\partial_z a = -\frac{1}{2n_0 k_0}\partial_x^2 a + \frac{k_0 n_2 |a|^2}{1 + |a|^2/I_{\rm sat}} a - \frac{i}{\Lambda_{\rm abs}} a, \tag{2}$$

where $n_0 \simeq 1$ is the linear index of refraction and $\Lambda_{\rm abs} = 30$ cm, which corresponds to a 60% transmission for a cell of length $L = 7.5$ cm. The value of the effective amplitude at the entrance of the cell is taken as

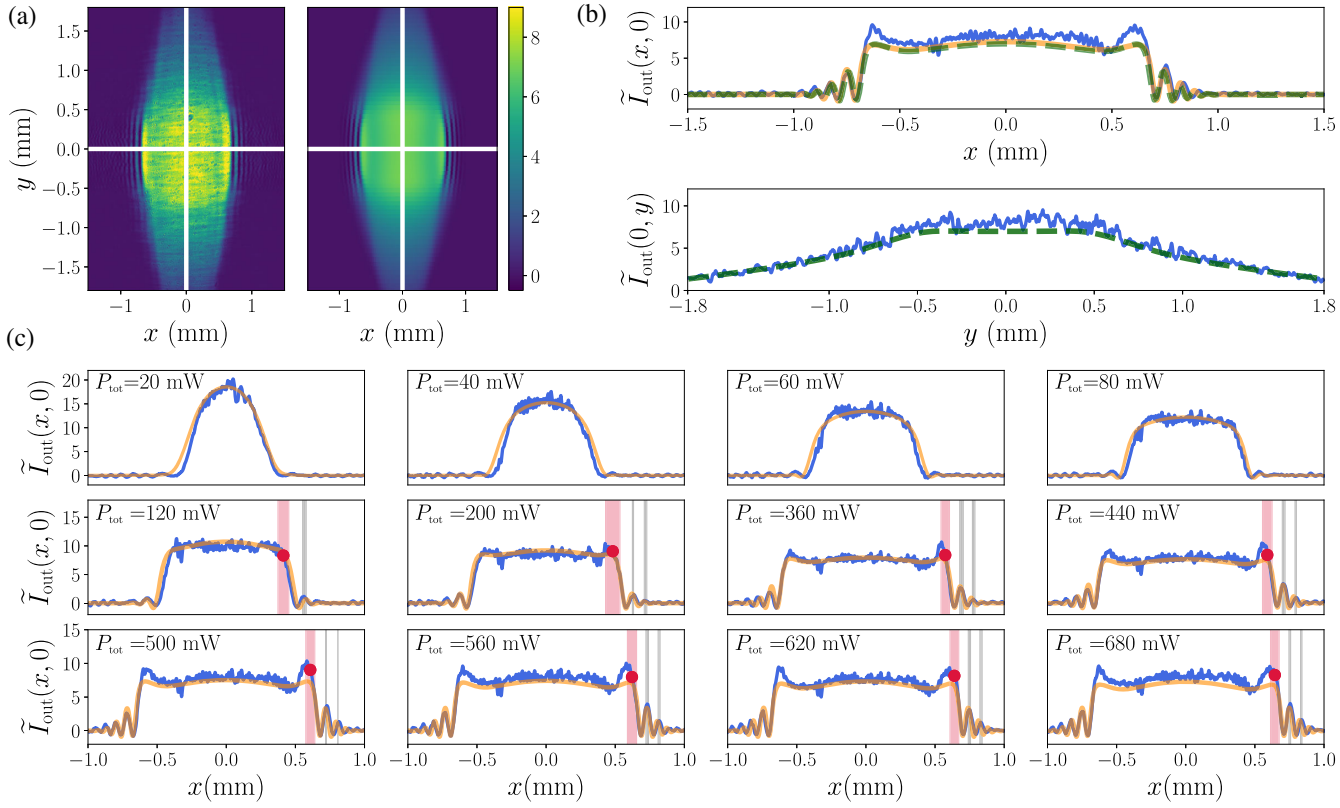


FIG. 2. (a) Left: experimental profile $\tilde{I}_{\rm out}$ taken for $P_{\rm tot} = 680$ mW. Right: Two-dimensional numerical simulations at the same total entrance power. (b) x and y profiles along the cuts represented by the two white lines on the two-dimensional profiles (a). The solid blue line represents the experimental data, the dashed green line the two-dimensional numerical simulation. On the x profile, the orange line is a one-dimensional numerical simulation, from Eqs. (2) and (3). (c) $\tilde{I}_{\rm out}(x,0)$ for various total beam powers. The color code is the same as in (b). The vertical pink and gray bars on the right part of each intensity profile indicate the positions of the solitonic edge of the DSW and of the first maxima of oscillations within the DSW. The thickness of each bar represents the experimental uncertainty.

$$a(x,0) = \sqrt{\mathcal{I}_0} + \sqrt{\mathcal{I}_1}\exp\left(-\frac{x^2}{w_{x,1}^2}\right). \tag{3}$$

In order to evaluate the accuracy of the mapping to the 1D model of Eq. (2), we compare in the upper panel of Fig. 2(b) the corresponding value of $|a(x,L)|^2\exp(2L/\Lambda_{\rm abs})/\mathcal{I}_0 - 1$ with the experimental $\tilde{I}_{\rm out}(x,0)$ and with the result of 2D simulations. The excellent agreement is confirmed in Fig. 2(c) for the whole range of beam powers $P_{\rm tot}$.

The mapping to a 1D problem enables us to compare our measurements with recent analytical predictions. In particular, if one neglects the linear absorption within the cell, for the initial intensity profile (3), wave breaking occurs at a propagation distance [45]

$$z_{WB} = 4\sqrt{\frac{n_0 I^*}{n_2}}\frac{(1+I^*/I_{\rm sat})^2}{3+I^*/I_{\rm sat}}\cdot\frac{1}{\max\left|\frac{dI(x,0)}{dx}\right|}, \tag{4}$$

where $I(x,0) = |a(x,0)|^2$ is the entrance intensity and I^* is the value $I(x^*,0)$ at point x^*, where $|dI(x,0)/dx|$ reaches its maximum. For low entrance power, no DSW is observed because z_{WB} is larger than the cell length. Wave breaking first occurs within the cell for a total power P_{WB} such that $z_{WB} = L$. For our experimental parameters we obtain $P_{WB} = 48$ mW. Numerical tests show that taking absorption into account does not modify notably this value.

For a total power larger than P_{WB}, the DSW is formed and develops within the cell. The physical phenomenon at the origin of the DSW is the following: large intensity perturbations propagate faster than small ones, so there exist values of x reached at the same "time" by different intensities. When this occurs first, the density gradient is infinite. This corresponds to the onset of a cusp catastrophe [54,62], the nonlinear diffractive dressing of which is a dispersive shock wave. This takes the form of a modulated oscillating pattern consisting asymptotically (i.e., at large z, or equivalently large $P_{\rm tot}$) in a train of solitons which, away from the center of the beam, gradually evolves into a linear perturbation. The position of its "solitonic edge" on the $y = 0$ axis at the cell output ($z = L$) is denoted as x_s. It is located in Figs. 2(c) by a vertical red bar whose thickness represents the uncertainty on the estimation of x_s from the experimental $\tilde{I}_{\rm out}(x,0)$. This uncertainty limits the

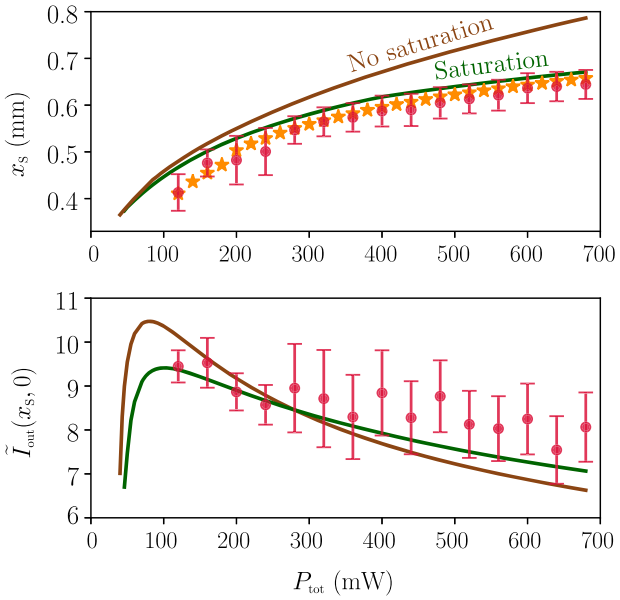


FIG. 3. Characterization of the solitonic edge of the DSW as a function of the beam's power. The upper panel represents the position x_s of the shock, and the lower one the corresponding intensity $\tilde{I}_{\rm out}(x_s, 0)$. In each panel, the red points with error bars are experimental results, from Fig. 2(c) and, in the upper one, the orange stars are the results of 1D numerical simulations of Eq. (2). The green solid line is the theoretical result, from Ref. [47]. The brown solid line is the theoretical result in the absence of saturation.

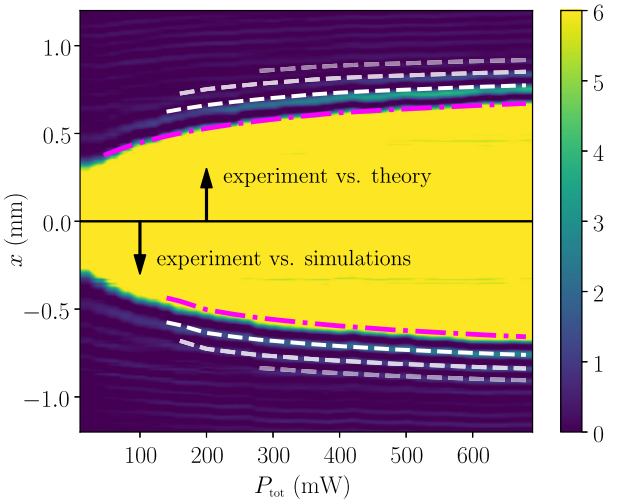


FIG. 4. Color plot of the experimental intensity profiles $\tilde{I}_{\rm out}(x, 0)$ as a function of $P_{\rm tot}$. The purple dot-dashed line represents the edge x_s of the DSW extracted from Whitham theory (upper part of the figure: $x > 0$) and from 1D numerical simulations (lower part, $x < 0$). In each half of the figure ($x \lessgtr 0$) the white dashed lines are the corresponding analytic predictions (5) for the maxima of oscillation.

experimental determination of x_s to powers larger than 120 mW. The following maxima of oscillations, represented by vertical gray lines, are more precisely determined experimentally. The technique devised in Ref. [47] makes it possible to theoretically determine x_s and the corresponding intensity $\tilde{I}_{\rm out}(x_s, 0)$. As illustrated in Fig. 3 the results of this analytical approach (green solid lines) compare well with the experimental data, although it does not take absorption into account. Importantly, omission of the nonlinearity saturation leads to incorrect results (brown solid line).

One may study the DSW in an even more detailed way by locating the position of the maxima of the nonlinear oscillations. While the theoretical results for x_s essentially rely on an approach due to El [34,40,43] which is valid for any type of nonlinearity, the precise intensity profile within the DSW can be computed only for exactly integrable systems, i.e., by neglecting saturation effects. The position-dependent oscillation period $\mathcal{L}(x, z)$ was computed in this framework in Ref. [46] for a parabolic initial intensity distribution. Fitting the center of the intensity profile (3) by an inverted parabola, the positions x_1, x_2, and x_3 of the first maxima of oscillation of the DSW at the output of the cell are determined by

$$x_1 - x_s = \mathcal{L}\left(\frac{x_s + x_1}{2}, L\right), \tag{5}$$

and by similar formulas obtained by replacing x_1 by x_2 (then x_3) and x_s by x_1 (then x_2). The results are compared with the experimental ones in the upper half ($x > 0$) of Fig. 4. The small offset in the position of the theoretical maxima with respect to the experimental ones observed in the figure is due to an initial small overshoot in the theoretical position of x_s (cf. the green solid line in Fig. 3) which is itself due to the absence of absorption in the model. Indeed, the 1D numerical simulations—which do take absorption into account—are in slightly better agreement with the experimental results for x_s (cf. the orange stars in Fig. 3). Using the numerical x_s in Eq. (5) instead of the analytical one yields, for the maxima of oscillations, an excellent agreement with experiment, cf. the lower half of Fig. 4. Such a good agreement despite the fact that Eq. (5) does not take saturation into account is not surprising: the rapid decrease of intensity away from the solitonic edge (cf. Fig. 2) significantly reduces the importance of saturation within the DSW.

It thus appears possible to give a detailed description of precise experimental recordings of the intensity pattern of an optical shock wave, not only thanks to numerical simulations, but on the basis of Whitham's modulation theory. This is an important validation of recent advances in this approach, which is no longer restricted to integrable systems or idealized initial configurations. We are reaching a point where these progresses make it possible not only to study DSWs *per se*, but also as tools for prospecting new physical phenomena, such as the type of wave-mean flow interaction recently identified in Ref. [55]: our platform is ideally designed to investigate scattering of elementary

excitations by a DSW, a study which is also relevant to the domain of analogue gravity. Indeed, as discussed in the Supplemental Material [53], a dispersive shock can be considered as an exotic model of acoustic white hole, and the good experimental control and theoretical understanding of this structure demonstrated in the present work opens the prospect of a detailed investigation of the corresponding induced background fluctuations.

T. B. would like to thank Russel Bisset for stimulating discussions about the numerical methods. This work received funding from the European Union Horizon 2020 research and innovation programme under grant agreement No. 820392 (PhoQuS) and from the Region Île-de-France in the framework of DIM SIRTEQ (HydroLive). Q. G. and A. B. thank the Institut Universitaire de France (IUF) for support.

[1] S. N. Gurbatov, O. V. Rudenko, and A. I. Aaichev, *Waves and Structures in Nonlinear Nondispersive Media, General Theory and Applications to Nonlinear Acoustics* (Springer-Verlag, Berlin and Heidelberg, 2011).
[2] A. Jeffrey and T. Taniuti, *NonLinear Wave Propagation with Applications to Physics and Magnetohydrodynamics* (Academic Press, London, 1964).
[3] A. J. C. Barré de Saint-Venant, Théorie du mouvement non permanent des eaux, avec application aux crues des rivières et à l'introduction de marées dans leurs lits, C.R. Hebd. Seances Acad. Sci. **73**, 147 and 237 (1871).
[4] H. Lacombe and M. Bellevaux, Courants de densité dans le détroit de Gibraltar, La Houille Blanche **1**, 38 (1965).
[5] L. V. Ovsyannikov, Two-layer shallow water model, J. Appl. Mech. Tech. Phys. **20**, 127 (1979).
[6] S. A. Akhmanov, A. P. Sukhorukov, and R. V. Khokhlov, Self-focusing and self-trapping of intense light beams in a nonlinear medium, Sov. Phys. JETP **25**, 1025 (1966).
[7] Y. Kagan, E. L. Surkov, and G. V. Shlyapnikov, Evolution of a Bose-condensed gas under variations of the confining potential, Phys. Rev. A **54**, R1753 (1996).
[8] Y. Castin and R. Dum, Bose-Einstein Condensates in Time Dependent Traps, Phys. Rev. Lett. **77**, 5315 (1996).
[9] J. A. Joseph, J. E. Thomas, M. Kulkarni, and A. G. Abanov, Observation of Shock Waves in a Strongly Interacting Fermi Gas, Phys. Rev. Lett. **106**, 150401 (2011).
[10] S. Datta and U. R. Fischer, Fluid-dynamical analogue of nonlinear gravitational wave memory, arXiv:2011.05837.
[11] B. Riemann, On the propagation of planar air waves of finite amplitude, in *Collected papers* (Kendrick Press, Heber City, 2004).
[12] R. Courant and K. O. Friedrichs, *Supersonic Flow and Shock Waves, a Manual on the Mathematical Theory of Non-Linear Wave Motion* (Scholar's Choice, Wolcott, 2015).
[13] Y. B. Zel'dovich and Y. P. Raizer, *Physics of Shock Waves and High-Temperature Hydrodynamic Phenomena* (Dover, New York, 2002).
[14] R. Z. Sagdeev, Cooperative phenomena and shock waves in collisionless plasmas, in *Reviews of Plasma Physics*, Vol. 4, edited by M. A. Leontovich (Consultants Bureau, New York, 1966), p. 23.
[15] A. V. Gurevich and L. P. Pitaevskii, Nonstationary structure of a collisionless shock wave, Sov. Phys. JETP **38**, 291 (1973).
[16] G. B. Whitham, Non-linear dispersive waves, Proc. R. Soc. A **283**, 238 (1965).
[17] J. E. Rothenberg and D. Grischkowsky, Observation of the Formation of an Optical Intensity Shock and Wave Breaking in the Nonlinear Propagation of Pulses in Optical Fibers, Phys. Rev. Lett. **62**, 531 (1989).
[18] G. Couton, H. Maillotte, and M. Chauvet, Self-formation of multiple spatial photovoltaic solitons, J. Opt. B **6**, S223 (2004).
[19] W. Wan, S. Jia, and J. W. Fleischer, Dispersive superfluid-like shock waves in nonlinear optics, Nat. Phys. **3**, 46 (2007).
[20] S. Jia, W. Wan, and J. W. Fleischer, Dispersive Shock Waves in Nonlinear Arrays, Phys. Rev. Lett. **99**, 223901 (2007).
[21] N. Ghofraniha, C. Conti, G. Ruocco, and S. Trillo, Shocks in Nonlocal Media, Phys. Rev. Lett. **99**, 043903 (2007).
[22] C. Barsi, W. Wan, C. Sun, and J. W. Fleischer, Dispersive shock waves with nonlocal nonlinearity, Opt. Lett. **32**, 2930 (2007).
[23] N. Ghofraniha, S. Gentilini, V. Folli, E. DelRe, and C. Conti, Shock Waves in Disordered Media, Phys. Rev. Lett. **109**, 243902 (2012).
[24] M. Elazar, V. Fleurov, and S. Bar-Ad, All-optical event horizon in an optical analog of a laval nozzle, Phys. Rev. A **86**, 063821 (2012).
[25] N. Ghofraniha, L. Santamaria Amato, V. Folli, S. Trillo, E. DelRe, and C. Conti, Measurement of scaling laws for shock waves in thermal nonlocal media, Opt. Lett. **37**, 2325 (2012).
[26] J. Fatome, C. Finot, G. Millot, A. Armaroli, and S. Trillo, Observation of Optical Undular Bores in Multiple Four-Wave Mixing, Phys. Rev. X **4**, 021022 (2014).
[27] G. Xu, A. Mussot, A. Kudlinski, S. Trillo, F. Copie, and M. Conforti, Shock wave generation triggered by a weak background in optical fibers, Opt. Lett. **41**, 2656 (2016).
[28] B. Wetzel, D. Bongiovanni, M. Kues, Y. Hu, Z. Chen, S. Trillo, J. M. Dudley, S. Wabnitz, and R. Morandotti, Experimental Generation of Riemann Waves in Optics: A Route to Shock Wave Control, Phys. Rev. Lett. **117**, 073902 (2016).
[29] G. Xu, M. Conforti, A. Kudlinski, A. Mussot, and S. Trillo, Dispersive Dam-Break Flow of a Photon Fluid, Phys. Rev. Lett. **118**, 254101 (2017).
[30] J. Nuño, C. Finot, G. Xu, G. Millot, M. Erkintalo, and J. Fatome, Vectorial dispersive shock waves in optical fibers, Commun. Phys. **2**, 138 (2019).
[31] J.-L. Coutaz and M. Kull, Saturation of the nonlinear index of refraction in semiconductor-doped glass, J. Opt. Soc. Am. B **8**, 95 (1991).
[32] Y. S. Kivshar and G. P. Agrawal, *Optical Solitons, From Fibers to Photonic Crystals* (Academic, New York, 2003).
[33] A. V. Gurevich and A. L. Krylov, Dissipationless shock waves in media with positive dispersion, Sov. Phys. JETP **65**, 944 (1987).

[34] A. V. Gurevich and A. P. Meshcherkin, Expanding self-similar discontinuities and shock waves in dispersive hydrodynamics, Sov. Phys. JETP **60**, 732 (1984).
[35] A. V. Gurevich, A. L. Krylov, and N. G. Mazur, Quasisimple waves in Korteweg-de Vries hydrodynamics, Sov. Phys. JETP **68**, 966 (1989).
[36] A. L. Krylov, V. V. Khodorovskii, and G. A. El, Evolution of a nonmonotonic perturbation in Korteweg-de Vries hydrodynamics, JETP Lett. **56**, 323 (1992).
[37] G. A. El and V. V. Khodorovsky, Evolution of a solitonless large-scale perturbation in Korteweg-de Vries hydrodynamics, Phys. Lett. A **182**, 49 (1993).
[38] G. A. El and A. L. Krylov, General solution of the Cauchy problem for the defocusing NLS equation in the Whitham limit, Phys. Lett. A **203**, 77 (1995).
[39] Y. Kodama, The Whitham equations for optical communications: Mathematical theory of NRZ, SIAM J. Appl. Math. **59**, 2162 (1999).
[40] G. A. El, Resolution of a shock in hyperbolic systems modified by weak dispersion, Chaos **15**, 037103 (2005).
[41] G. A. El, A. Gammal, E. G. Khamis, R. A. Kraenkel, and A. M. Kamchatnov, Theory of optical dispersive shock waves in photorefractive media, Phys. Rev. A **76**, 053813 (2007).
[42] M. G. Forest, C.-J. Rosenberg, and O. C. Wright, On the exact solution for smooth pulses of the defocusing nonlinear Schrdinger modulation equations prior to breaking, Nonlinearity **22**, 2287 (2009).
[43] A. M. Kamchatnov, Dispersive shock wave theory for nonintegrable equations, Phys. Rev. E **99**, 012203 (2019).
[44] M. Isoard, A. M. Kamchatnov, and N. Pavloff, Long-time evolution of pulses in the Korteweg–de Vries equation in the absence of solitons reexamined: Whitham method, Phys. Rev. E **99**, 012210 (2019).
[45] M. Isoard, A. M. Kamchatnov, and N. Pavloff, Dispersionless evolution of inviscid nonlinear pulses, Europhys. Lett. **129**, 64003 (2020).
[46] M. Isoard, A. M. Kamchatnov, and N. Pavloff, Wave breaking and formation of dispersive shock waves in a defocusing nonlinear optical material, Phys. Rev. A **99**, 053819 (2019).
[47] S. K. Ivanov, J.-E. Suchorski, A. M. Kamchatnov, M. Isoard, and N. Pavloff, Formation of dispersive shock waves in a saturable nonlinear medium, Phys. Rev. E **102**, 032215 (2020).
[48] N. Šantić, A. Fusaro, S. Salem, J. Garnier, A. Picozzi, and R. Kaiser, Nonequilibrium Precondensation of Classical Waves in Two Dimensions Propagating Through Atomic Vapors, Phys. Rev. Lett. **120**, 055301 (2018).
[49] C. Michel, O. Boughdad, M. Albert, P.-E. Larré, and M. Bellec, Superfluid motion and drag-force cancellation in a fluid of light, Nat. Commun. **9**, 2108 (2018).
[50] Q. Fontaine, T. Bienaimé, S. Pigeon, E. Giacobino, A. Bramati, and Q. Glorieux, Observation of the Bogoliubov Dispersion in a Fluid of Light, Phys. Rev. Lett. **121**, 183604 (2018).
[51] Q. Fontaine, P.-E. Larré, G. Lerario, T. Bienaimé, S. Pigeon, D. Faccio, I. Carusotto, E. Giacobino, A. Bramati, and Q. Glorieux, Interferences between Bogoliubov excitations in superfluids of light, Phys. Rev. Research **2**, 043297 (2020).
[52] O. Boughdad, A. Eloy, F. Mortessagne, M. Bellec, and C. Michel, Anisotropic nonlinear refractive index measurement of a photorefractive crystal via spatial self-phase modulation, Opt. Express **27**, 30360 (2019).
[53] See Supplemental Material at http://link.aps.org/supplemental/10.1103/PhysRevLett.126.183901 which presents our 2D numerical simulations, discusses the analogy of a dispersive shock with a white hole, and includes Refs. [54–60].
[54] A. M. Kamchatnov, *Nonlinear Periodic Waves and Their Modulations: An Introductory Course* (World Scientific, Singapore, 2000).
[55] T. Congy, G. A. El, and M. A. Hoefer, Interaction of linear modulated waves and unsteady dispersive hydrodynamic states with application to shallow water waves, J. Fluid Mech. **875**, 1145 (2019).
[56] G. El, V. Geogjaev, A. Gurevich, and A. Krylov, Decay of an initial discontinuity in the defocusing NLS hydrodynamics, Physica (Amsterdam) **87D**, 186 (1995).
[57] A. V. Gurevich and L. P. Pitaevskii, Averaged description of waves in the Korteweg-de Vries-Burgers equation, Sov. Phys. JETP **66**, 490 (1987).
[58] V. V. Avilov, I. M. Krichever, and S. P. Novikov, Evolution of Whitham zone in the theory of Korteweg-de Vries, Sov. Phys. Dokl. **32**, 564 (1987).
[59] A. Kamchatnov, On Whitham theory for perturbed integrable equations, Physica (Amsterdam) **188D**, 247 (2004).
[60] P.-E. Larré, N. Pavloff, and A. M. Kamchatnov, Wave pattern induced by a localized obstacle in the flow of a one-dimensional polariton condensate, Phys. Rev. B **86**, 165304 (2012).
[61] L. D. Landau and E. M. Lifshitz, *Electrodynamics of Continuous Media, Volume 8 (Course of Theoretical Physics)* (Pergamon Press, New York, 1984).
[62] M. Golubitsky, An introduction to catastrophe theory and its applications, SIAM Rev. **20**, 352 (1978).